Biocompatibility, thermal and mechanical properties of glass fiber-reinforced polybenzoxazine composites as a potential new endodontic post

Journal:	*Polymer Composites*
Manuscript ID	PC-24-2172.R1
Wiley - Manuscript type:	Research Article
Date Submitted by the Author:	20-Jul-2024
Complete List of Authors:	Mora, Phattarin; Srinakharinwirot University - Ongkharak Campus Rimdusit, Sarawut; Chulalongkorn University Karagiannidis, Panagiotis; University of Sunderland Srisorrchart, Ukrit; Institute of Dentistry Jubsilp, Chanchira; Srinakharinwirot University - Ongkharak Campus
Keywords:	composites, dental polymers, biocompatibility, thermal properties, simulations

Biocompatibility, thermal and mechanical properties of glass fiber-reinforced polybenzoxazine composites as a potential new endodontic post

Phattarin Mora[1], Sarawut Rimdusit[2], Panagiotis Karagiannidis[3], Ukrit Srisorrchart[4], Chanchira Jubsilp[1]

[1]Department of Chemical Engineering, Faculty of Engineering, Srinakharinwirot University, Nakhonnayok 26120, Thailand.

[2]Center of Excellence in Polymeric Materials for Medical Practice Devices, Department of Chemical Engineering, Faculty of Engineering, Chulalongkorn University, Bangkok 10330, Thailand.

[3]School of Engineering, Faculty of Technology, University of Sunderland, Sunderland, SR6 0DD, United Kingdom.

[4]Institute of Dentistry, Department of Medical Services, Nonthaburi 11000, Thailand

Correspondence : E-mail: chanchira@g.swu.ac.th

Abstract

A novel dental fiber post from glass fiber-reinforced polybenzoxazine (PBZ) composites was developed in this work. The essential properties, i.e., chemical characteristics, thermal and biological properties of the PBZ composites were investigated for various glass fiber loadings (10.5, 23.7, 41.2 and 65.1 vol%). Finite element analysis (FEA) was also utilized to observe mechanical behaviours of the tooth model repaired with PBZ composite posts compared to a natural tooth model. The findings reveal that for the fiber-reinforced PBZ composites not only their thermal properties were significantly improved, but they also showed enhanced cytocompatibility; we found a coefficient of thermal expansion of 12.8 ppm/^{o}C and cell viability of 91.55 for the 65.1 vol% glass fiber-reinforced PBZ composite. Moreover, samples reinforced with higher glass fiber loadings effectively resulted in the reduction of stress distribution in dentin observed from FEA suggesting protection againt root fractures. Restoration using the PBZ composite post showed the same stress patterns in the dentin-composite resin-post interface of the repaired tooth as in the natural tooth model. The results revealed that the glass fiber-reinforced PBZ composites possess good thermal properties and mechanical behaviours which renders them suitable candidates for biocompatible dental materials.

Highlights

- The GF/polybenzoxazine composites had nontoxic properties as evidenced through cell viability, growth and morphology studies.
- The thermal expansion of the GF/polybenzoxazine composite was similar to that of dentin, promoting adaptation at the dentin-post interface.
- Mechanical behaviors evaluated by FEA of tooth model restored with GF/polybenzoxazine composite post were similar to those restored with commercial glass fiber post.
- The biocompatible GF/polybenzoxazine composite with good thermal and mechanical properties is a promising new candidate material as dental fiber post.

KEYWORDS

composite dental post, polybenzoxazine composite, biocompatible material, thermoset polymer, innovation

1 INTRODUCTION

Fiber reinforced polymer composites (FRPs) based on carbon, aramid or glass fibers have been widely used in automotive, airspace, defence and marine engineering industries,[1-8] and have been more recently used as biomedical materials in dentistry as dental fiber post for endodontically treated teeth. Patients with intrinsic or extrinsic stains need dental restorations to address aesthetic issues, e.g., antibiotics and smoking habits, in consequent, a reinforcing structure which is known as post is often used for the dental restorations.[9-11] Generally, the post materials should impart good retention without overstressing root dentin and should have properties close to those of dentin, including elastic modulus, flexural and compressive strength, and thermal expansion and they also should be able to bond efficiently to the dentin.[12] These characteristics can help to ensure that the post and dentin perform in a similar manner and reduce the risk of failure. Non-metallic posts have been gradually replacing regular metallic posts in recent years due to the disadvantages of metals, i.e., high elastic modulus, approximately 100-200 GPa, resulting in generation of stress concentration areas, which were responsible for cracking and root fracture, and the risk of corrosion.[10,13-15] Therefore, non-metallic posts, e.g., fiber posts (fiber-reinforced epoxy posts) and ceramic posts have become gradually current in dentistry due to their usefulness such as ease of treatment, optimal mechanical properties, aesthetics, removability, and their ability to provide probable clinical

performance in several respects. Contrary to metallic posts, fiber posts have a stiffness closer to dentin which has elastic modulus of 18.6-40 GPa, and thus minimize the root fracture risk.[15,16] In addition, significant bonding of fiber posts to dentin and to a composite core creates better stress distribution and transfer after loading, leading to improve root's fracture resistance.[17]

Carbon fiber posts (CF-reinforced epoxy posts) were firstly adequate replacements to metal posts (custom and prefabricated) because the posts had a stiffness like dentin and were easy to remove. However, the CF posts have higher strength than other fiber posts and are black and opaque, therefore lacking cosmetic qualities. In recent years, glass fiber (GF) posts were introduced as an innovative material to replace unaesthetic CF posts in the repair of teeth that have had endodontic therapy due to its advantages especially its elastic modulus and strength like dentin, providing uniform stress distribution along the post length. GF posts also show convenience in aesthetic appearance, they are competitive and have a lower risk of further tooth structure loss during post-space preparation.[18,19] Different prefabricated fiber-reinforced posts have been studied and exhibited variations in mechanical properties.[19] The flexural properties of FRP posts, i.e., GF, CF and quartz fiber posts, were compared against a brass post. It was found that the CF post showed the highest flexural modulus about 100 GPa, while the flexural modulus of GF posts was in a range of 2.28-30.30 GPa, depending on diameter and aspect ratio of the fibres used to prepare the post. The flexural moduli of quartz fiber and brass posts were about 8.80 GPa and 15.12 GPa, respectively. A low modulus which is equal to that of dentin may avoid stress concentrations and prevent additional root fractures. In addition, the GF post achieved the highest flexural strength when compared to the CF post. This indicates that the GF post can enhance the durability to retain the core of the restoration.[20] Pegoretti et al.[21] analysed through FEA the mechanical response of tooth repaired with GF-reinforced polymer composite post and compared against tooth repaired with CF and gold alloy posts. Due to its rigidity which found similar to that of dentin, it was discovered that the composite post reinforced with GF expressed the lowest stresses inside the root.

In terms of polymer matrix for dental fiber posts, epoxy and bis-GMA were the most used polymer matrices, while investigations were also conducted using other polymers such as polyimide and PEEK.[21-23] In case of the epoxy matrix, its curing agents such as amines, present various drawbacks, including issues like inadequate storage stability and high toxicity. Additionally, epoxy resin is known for its poor heat resistance, evident in its low glass transition temperature (T_g) and limited thermal expansion.[24,25] To find alternatives to the use of a highly toxic curing agent in epoxy resin, in recent years, Mora et al.[26] presented fiber posts

prepared from GF and polybenzoxazine (PBZ). PBZ, a new type of thermoset phenolics, has some outstanding properties, e.g., high thermal and mechanical properties, low water absorption and good solvent resistance. The benzoxazine monomer can be produced by a patented solventless synthesis from formaldehyde, primary amines, and phenols, providing high purity monomers, with low melt viscosity which facilitate compounding with different fillers such as fibers and offers enormous molecular design flexibility by alloying with several types of polymers for broader range of applications. In addition, ring-opening polymerization of the benzoxazine monomer under thermal conditions without adding curing agents and catalysts was stated.[27-30] Mora et al.[26] reported GF-reinforced PBZ composites which had the necessary essential properties for dental restorations and appliances since the flexural properties of the GF-reinforced PBZ composite were found to be similar to that of dentin. This performance suggested that a critical factor for load transfer which is the difference in rigidity between the PBZ composite and the dentin was reduced. Because of good adhesion at GF-PBZ interface, the T_g of the PBZ composite was noticeably greater than that of the PBZ. The higher T_g of the composite is important for long term thermal stability for dental restorations. Moreover, it was found from FEA that the maximum von Mises stress under an oblique applied load showed at the cervical third area for the tooth model repaired with the PBZ composite post as equally observed in the natural tooth model. However, thermal performance, i.e., thermal expansion and degradation temperature, and biological property of the GF-reinforced PBZ composite post as well as the mechanical behaviour under a vertical load to mimic bruxism of tooth model repaired with the composite post by FEA is not reported yet in literature to emphasize the advantage of using the GF-reinforced PBZ composite as a dental fiber post.

Therefore, this study aimed to prepare a biocompatible dental fiber post using bisphenol A/aniline-type PBZ (PBA-a) composites reinforced with GF. The effect of GF loading on thermal expansion, degradation temperature, and biocompatibility was studied in this work. The stress distribution in a tooth model repaired with the obtained GF-reinforced PBA-a composite posts after applying a vertical load was compared with a natural tooth model. Moreover, the improved properties of the composites obtained due to chemical bond formation were also discussed.

2 MATERIALS AND METHODS

2.1 Materials

Bisphenol A/aniline-type benzoxazine (BA-a) resin was used as the matrix to formulate GF-reinforced composites. Aniline and paraformaldehyde were acquired from Panreac Quimica and Merck Co., Ltd., respectively. Bisphenol-A was supplied by Thai Polycarbonate Co., Ltd. Plain weave of GF with areal density of 600 g/cm^2 was used as reinforcing fiber obtained from Thai Polyadd Ltd. Partnership.

2.2 Resin and sample preparation

BA-a resin polymerized to be PBA-a was produced from aniline, paraformaldehyde and bisphenol-A at a molar ratio of 2:4:1 based on a solventless method.[27]

The GF/PBA-a composites were prepared as illustrated in Figure 1 using different GF loading levels of 0, 10.5, 23.7, 41.2 and 65.1 % by volume. The obtained molten BA-a was coated on GF using hand-layup method at 80 °C to fabricate the prepregs. The GF/PBA-a composite was obtained by preheating at 180 °C for 1 h and followed by curing at 200 °C and 15 MPa in a compression molder for 2 h. To characterize the samples, they were all air-cooled to 25 °C in an open mold and then cut into the appropriate shapes using a diamond blade.

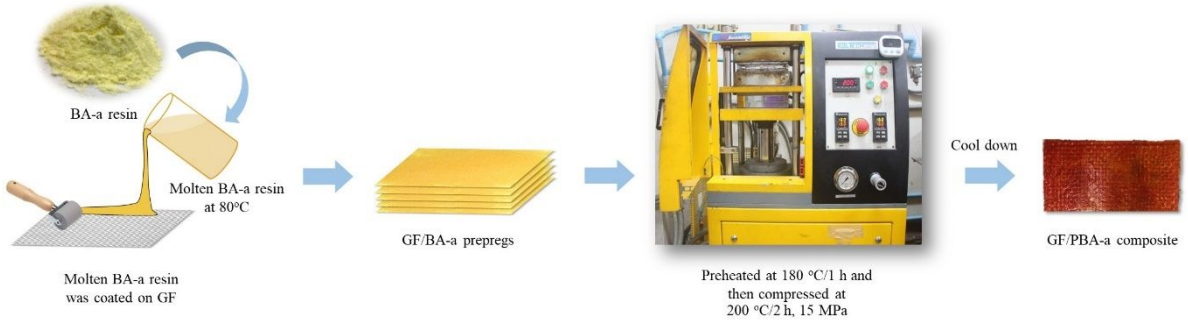

FIGURE 1 Preparation of GF/PBA-a composites.

2.3 Samples characterization

A thermomechanical analyzer (TMA) (Bruker-AXS, TMA 4010) was used to measure the coefficient of linear thermal expansion (CTE) of the samples. The samples with dimensions of 10 × 5 × 4 mm^3 were tested at a heating rate of 5 °C/min as an average value within 100 °C-200 °C with a fixed load of 5 mN (0.5 g) in a nitrogen atmosphere. The CTE of each sample was calculated by averaging three readings.

The thermal stability of the samples was investigated by a thermogravimetric analyzer (TGA) (model TGA1 STARe System, Mettler-Toledo). Samples between 5 to 10 mg were tested at a heating rate of 20 °C/min from 800 °C under nitrogen flow (50 mL/min). The results were verified by repeating three measurements pre sample.

FTIR spectra of the samples were collecting using a Spectrum GX FTIR spectrometer with an ATR accessory (Perkin Elmer instrument). 64 scans were used for each spectrum, with a spectral range from 4000 to 700 cm^{-1} and a resolution of 4 cm^{-1}. Each sample was analyzed in triplicate.

Cell viability tests incubated by standard in-vitro conditions at 37 ^{o}C for 24 h were performed on MC3T3-E1 cell-lines cultured by having 0.1% gelatin (+ive control).[31] The microplate reader (ELx-800) (Bio-Tek, Winooski) was used to capture the MC3T3-E1 cell lines. The complete medium without any samples and control sample, i.e., TritonX-100 in the medium was also performed to compare with the samples. The samples were analyzed in triplicate and the cell viability was determined using the Equation (1).

$$\text{Cell viability (\%)} = \frac{OD_S}{OD_C} \times 100\% \quad (1)$$

whereas: OD_S = sample concentration, OD_C = positive control

Statistical analysis was carried out using SPSS statistics software; cell viability assays were expressed as means ± SD (n=3). Comparisons between groups were performed with analysis of compare means (paired-samples T-Test). A $p < 0.05$ (ψ) and $p < 0.05$ (*) relative to complete medium and TritonX-100, respectively, was considered statistically significant.

To investigate the applied stresses on the tooth model repaired with a GF/PBA-a composite post, the stress distribution was derived using FEA. ANSYS Workbench 2022 R2 software, ANSYS Inc., was used to create two 3D models. All structures are included in the repaired tooth model as shown in Figure 2a. In comparison a natural tooth model is shown in Figure 2b. The 3D FEA of the models was meshed by structurally solid elements with the node and element numbers, i.e., 112,376 elements and 208,652 nodes for the treated tooth model, and 114,310 elements and 222,717 nodes for the natural tooth model. Constraints were imposed in all three directions as boundary conditions, making sure that rotating movements were permitted. It was determined that the model was isotropic, homogenous, and fully adherent. Elastic properties of the materials were used to define the mechanical properties of the model structures. All components were isotropic materials except for GF/PBA-a composite posts which are orthotropic materials. Their properties are tabulated in Tables 1 and 2, respectively.

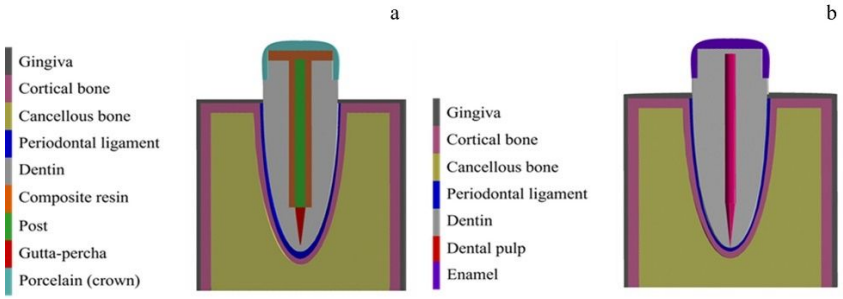

FIGURE 2 Schematics of tooth models: **a** tooth model repaired with the GF/PBA-a composite post, **b** natural tooth model.

TABLE 1 Elastic property of isotropic materials.

Material	Elastic modulus (GPa)	Poisson's ratio
Gingiva[21,32]	0.0196	0.03
Cortical bone[21,32]	13.7	0.30
Cancellous bone[32]	1.37	0.30
Periodontal ligament[21,32]	0.0689	0.45
Dentin[21,32]	18.6	0.31
Dental pulp[33]	0.002	0.45
Composite resin[34]	16.6	0.24
Gutta-percha[21,35]	0.00069	0.45
Porcelaine (Crown)[21,35]	120	0.28
Enamel[21,32]	41.0	0.30

TABLE 2 Elastic property of GF/PBA-a composite posts at different GF loadings and commercial glass fiber post.

GF/PBA-a composite posts	E_L (GPa)	$E_T = E_{T'}$ (GPa)	$G_{LT} = G_{LT'}$ (GPa)	$G_{TT'}$ (GPa)	$\nu_{LT} = \nu_{LT'}$	$\nu_{TL} = \nu_{T'L}$	$\nu_{TT'}$
10.5 vol% GF	10.9	6.78	2.37	2.55	0.28	0.17	0.33
23.7 vol% GF	17.1	8.88	3.01	3.35	0.26	0.14	0.33
41.2 vol% GF	23.0	12.70	4.22	4.89	0.24	0.14	0.30
65.1 vol% GF	28.0	21.78	7.28	8.69	0.22	0.17	0.25
Commercial GF post[36]	37.0	9.50	3.10	3.50	0.27	0.27	0.34

E_L (flexural modulus) of GF/PBA-a composite posts obtained from experimental,[26] while the other elastic properties are theoretical values evaluated from equations as shown in Pegoretti, et al.[21] with elastic modulus of PBA-a and glass fiber of 5.45 GPa and 72 GPa, respectively.

3 RESULTS AND DISCUSSION

3.1 Thermal compatibility of GF/PBA-a composites

The CTE of restorative materials for tooth restoration was studied because the materials expand upon heating by hot foods and drinks, while they can also be contracted when exposed to cold substances. The difference in CTE between the tooth and the restorative materials may result in fracture during their expansions and contractions. In order to function as a novel dental fiber post, GF/PBA-a composites are assessed for their CTE values. Figure 3a illustrates the displacement at a temperature range 20-150 °C of the GF/PBA-a composites at 0 vol% GF to 65.1 vol% GF. All the composites showed higher displacement when the temperature was increased. However, for a given temperature, the displacement of the sample was reduced with increasing GF loadings.

The average CTE value at the glassy region from 20 °C to 50 °C and from 20 °C to 150 °C of the PBA-a and the GF/PBA-a composites estimated from the slopes in Figure 3a are depicted in Figure 3. The CTE value in a range of 20-150 °C of the PBA-a was measured to be 60.0 ppm/°C. The addition of the reinforcement of GF into the PBA-a was found to decrease CTE of the PBA-a, i.e., CTE = 36. 3, 26.1, 18.7 and 13.3 ppm/°C for the composites reinforced with 10.5, 23.7, 41.2 and 65.1 vol% GF, respectively. At a temperature range of 20-50 °C, the CTE value of the PBA-a was also decreased with the increase of GF loading (CTE = 51.1 ppm/°C for PBA-a and CTE = 12.8 ppm/°C for 65.1 vol% GF). The reduction of the CTE values of the PBA-a composites with increasing amount of GF is due to the significantly lower CTE value of the GF, i.e., 5-12 ppm/°C[37] compared with that of the PBA-a. In addition, the more rigid structure of GF compared to PBZ matrix, i.e., the modulus of GF is 70-85 GPa,[38] might be causing a decreased motion of the macromolecule segments of the PBA-a, and the fiber-polymer matrix interfacial adhesion also plays a crucial role decreasing the CTE of the GF/PBA-a composites.[26,39] Consequently, to adopt the GF-reinforced PBA-a composite as a dental glass fiber post in tooth restoration, a comparison between the CTE values of the composites with the tooth matter such as dentin is more essential than the CTE value of each material. It was observed that the CTE values of the GF/PBA-a composite with 65.1 vol%, tended to reach the CTE of dentin, i.e., approximately 8.3-11.4 ppm/°C recorded in a temperature range of 20-50 °C[40] which is a typical tooth surface temperature during hot drink and food consumption.[41] Moreover, the CTE value of the composites with 65.1 vol% GF showed similarly to that of enamel (11.4 ppm/°C), composite resin (24-50 ppm/°C) and porcelain (12 ppm/°C).[42] Therefore, the CTE value of the 65.1 vol% GF/PBA-a composite was

in good agreement with that of dentin, resulting in less stress formation at the dentin-post interface, in consequence, preventing to loss of marginal adaptation.

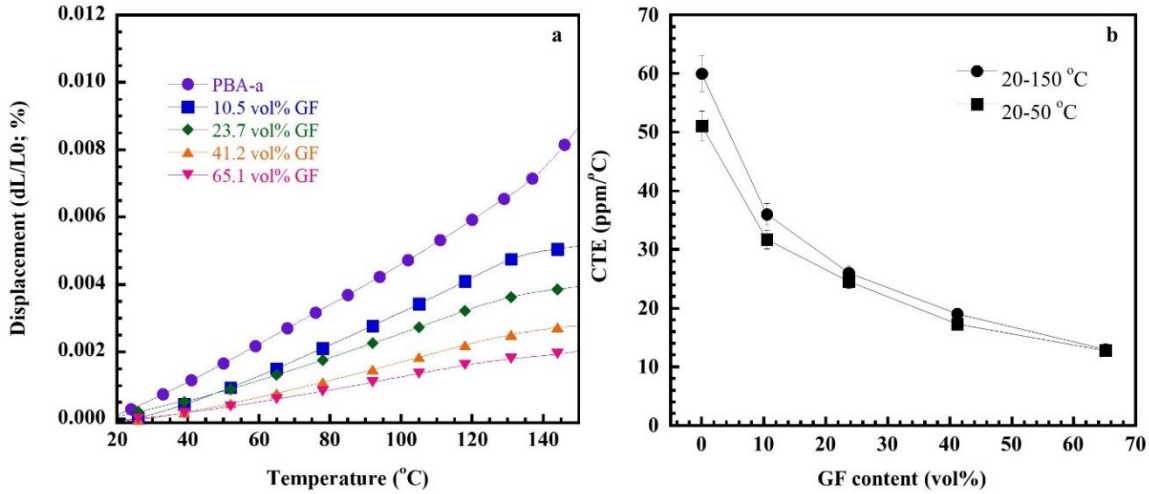

FIGURE 3 a TMA curves of PBA-a and GF/PBA-a composites at different GF loadings, **b** CTE of PBA-a and the composites in glassy region from 20 °C to 50 °C and from 20 °C to 150 °C

3.2 Thermal stability of GF/PBA-a composites

The thermal stability of restorative materials is necessary to understand the capability to tolerate the higher temperatures generated during tooth restoration without decomposition. TGA thermographs of the GF/PBA-a composites at different GF loadings are displayed in Figure 4a, while the numerical data, i.e., thermal degradation of weight loss at 5% (T_{d5}) and residual weight at 800 °C of the composites are depicted in Figure 4b.

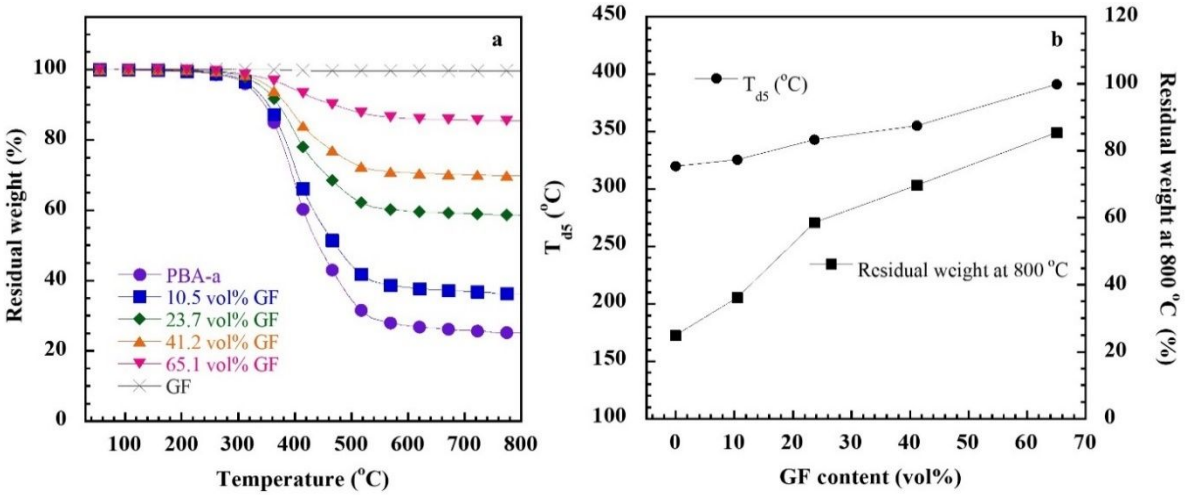

FIGURE 4 a TGA plot of GF, PBA-a and GF/PBA-a composites at different GF loadings, **b** T_{d5} and residual weight at 800 °C as a function of GF loading.

It was found that the T_{d5} of all composites increased from about 320 °C of the PBA-a to about 391 °C with the increase of the GF loading up to 65.1 vol%. The GF reinforcement in the PBA-a composites thus helps to increase thermal stability of the obtained GF/PBA-a composites since the degradation temperature of the GF is well above 1000 °C and the reinforcement of the GF can help to avoid the direct thermal degradation of the PBA-a by heat due to the GF shielding effect. In addition, the GF can also hinder the volatile organic compounds generated during thermal degradation of the PBA-a. For dental fiber post application, the T_{d5} of the developed composites was significantly greater than the thermal loading conditions of the human tooth surface approximately 15-50 °C for hot drink and food.

On the other hand, the residual weight at 800 °C of the GF/PBA-a composites (Figure 4b) was found to be 24 % for the PBA-a, while the residual weight of the composites was 36 % to 85 % with increasing GF loading (10.5 vol% up to 65.1 vol% GF). This characteristic is due to the mineral nature of GF which is naturally incombustible with no emitting toxic products when exposed to heat.

3.3 Biocompatibility of GF/PBA-a composites

The root canal restoration requires the materials used in the oral cavity to be nontoxic, chemically inert, and physically stable.[43] Therefore, in this work, in-vitro cell viability assay of GF/PBA-a composites were studied with MC3T3-E1 cell lines. The effect of GF loading in a range of 0-65.1 vol% on the cell viability and proliferation under standard in-vitro conditions was recorded over a period of 24 h after incubation.[44]

Figure 5 shows the maximum cell viability on the composite substrates at different GF loadings compared to that of complete medium and TritonX-100. The addition of the GF into PBA-a enhanced cell viability (%) of the PBA-a, i.e., 130.08 ± 0.02, 114.8 ± 0.02, 91.11 ± 0.02, 91.55 ± 0.03 for the composites with 10.5, 23.7, 41.2 and 65.1 vol% GF, respectively, while that of the PBA-a was 85.51 ± 0.02 %. This indicates that the GF imparts important physicochemical properties which facilitate cellular compatibility. It was also observed that some GF/PBA-a composites showed cell viability more than 100 %. This characteristic shows that PBA-a is possibly a non-toxic and biocompatible promoter. As a result, the developed GF/PBA-a composite showed that it could sustain cell survival and proliferation without endangering pre-osteoblastic cells. For statistical analysis in Figure 5, samples with $p < 0.05$ (ψ) are statistically significantly different when compared to complete medium for cell viability (%). At these GF loadings there was more than 14 % for cell growth of the 10.5 vol% and 23.7 vol% GF/PBA-a composites and less than 9 % for cell death of the 41.2 vol% GF/PBA-a

composite. Moreover, the significant difference was determined for all GF/PBA-a composites with $p < 0.05$ (*) versus TritonX-100. Cell growth was observed more than 14% in the composites reinforced with 10.5 and 23.7 vol% GF, while cell death was detected less than 9 % in the composites reinforced with 41.2 and 65.1 vol% GF. However, the cell viability of all GF/PBA-a composites was greater than 90 %, indicating the non-toxic nature of the material.

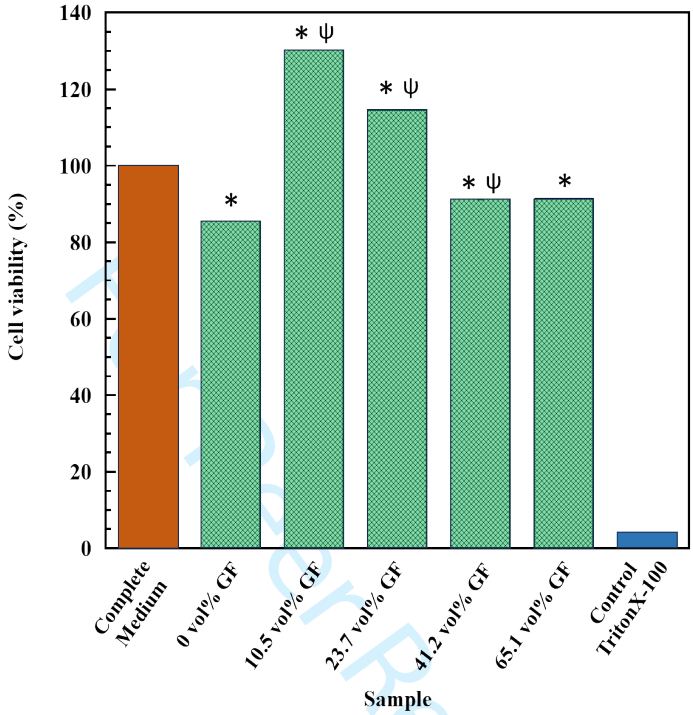

FIGURE 5 Cell viability of GF/PBA-a composites at different GF loadings.

Furthermore, the surface quality (i.e., chemistry, roughness and porosity) resulted in the cell viability with enhancing biocompatibility on the substrate surface, therefore, the MC3T3-E1 cell morphology was investigated against the GF/PBA-a composites at different GF loadings to determine their behaviour on cell growth and morphology as shown in Figure 6. Since PBA-a contains oxygen-based functional groups (hydroxyl groups, –OH) necessary for H-bonding, this resulted in an increased number of moieties were enhanced, which encouraged cell adhesion, differentiation, and growth.[45] Moreover, besides oxygen-based functional groups on the sample, the surface roughness is another important factor affecting cell adherence. The surface of the composites was much rougher, better interconnected, and more porous when GF was added that resulted in better cell adhesion over its surface.[46]

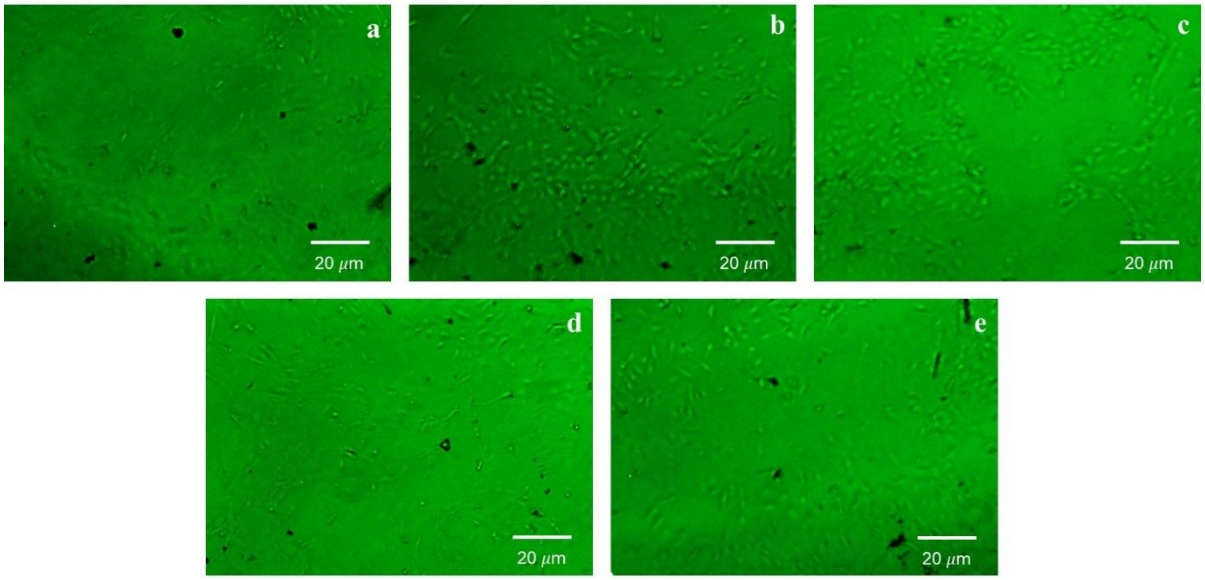

FIGURE 6 Cell morphology of MC3T3-E1 against GF/PBA-a composites at different GF loadings: **a** 0 vol%, **b** 10.5 vol%, **c** 23.7 vol%, **d** 41.2 vol%, **e** 65.1 vol%.

3.4 Finite element analysis of tooth model repaired with GF/PBA-a composite posts

FEA was used to investigate the use of the GF/PBA-a composites as a GF post. The distribution of von Mises stress (σ_v) on the tooth model repaired with posts, i.e., GF/PBA-a composite posts and commercial GF post[36], and on the natural tooth model is depicted in Figure 7. Moreover, the σ_v values at local coordinate system of the root at the cervical region patterned in Figure 8 are presented in Figure 9.

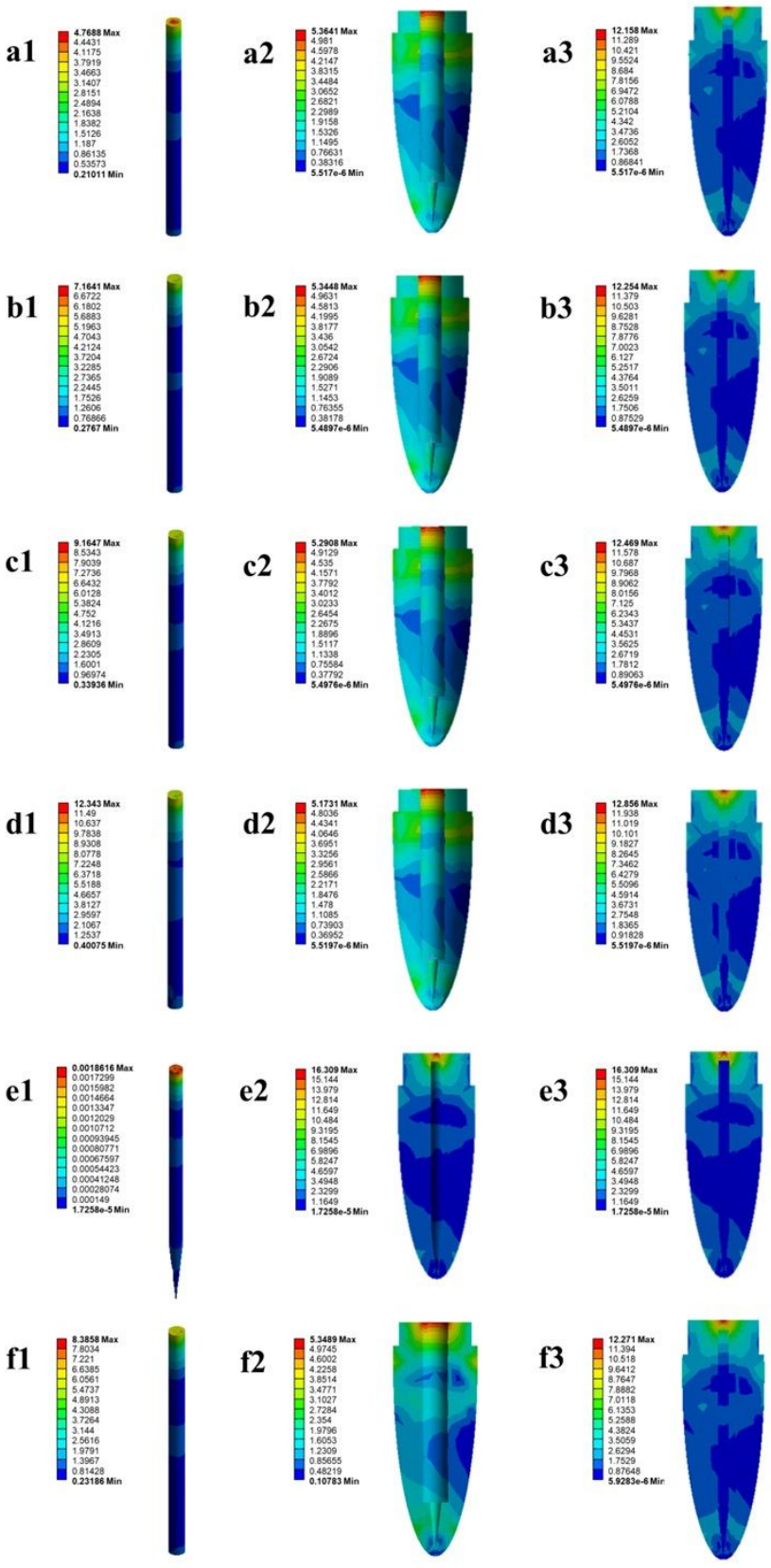

FIGURE 7 Stress patterns resulted from vertical load of 100 N applied on a tooth model repaired with GF/PBA-a composite post at different GF loadings: **a** 10.5 vol%, **b** 23.7 vol%, **c** 41.2 vol%, **d** 65.1 vol%, **e** natural tooth model, **f** tooth model repaired with commercial GF post[36] (**1**: σ_v at post, **2**: σ_v at dentin, **3**: σ_v of tooth model).

a

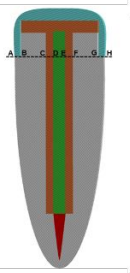

Path key point	Local coordinate (mm)
A	0.00
B	0.50
C	2.49
D	3.09
E	4.09
F	4.69
G	6.68
H	7.18

b

Path key point	Local coordinate (mm)
A	0.00
B	0.05
C	3.09
D	4.09
E	6.68
F	7.18

FIGURE 8 Tooth models and local coordinate systems: **a** tooth model repaired with post, **b** natural tooth model.

The σ_v distribution inside the post and at the interface is the most critical to prevent failure. As illustrated in Figures 7(a1)-7(d1), it was observed that higher σ_v values were distributed inside the developed composite post reinforced with higher GF loading as the maximum σ_v with 10.5, 23.7, 41.2, and 65.1 vol% GF was 4.7688, 7.1641, 9.1647 and 12.343 MPa, respectively. In other words, the maximum σ_v in the dentin for the tooth model repaired with the composite post with 10.5, 23.7, 41.2, and 65.1 vol% GF tended to decrease, i.e., 5.3641, 5.3448, 5.2908 and 5.1731 MPa, respectively. This was because the higher GF loading-reinforced composite post with a greater elastic modulus than that of the composite post with lower GF loading (as can be seen in Table 2) was probable to have larger stress from the root dentin than the composite post with lower elastic modulus, resulting in lower failure risk for higher elastic modulus of the composite post.

The stress patterns of the tooth model repaired with the GF/PBA-a composite posts can be seen in Figures 7(a3)-7(d3), and are compared to against those of the natural tooth model (Figure 7(e3)) and for the tooth model repaired with commercial GF post (Figure 7(f3)). It was observed that the stress patterns in the tooth model repaired with developed composite posts were in the closest resemblance to that of natural tooth model with maximum stress observed in the cervical third area dissipating as the stresses travel apically. This pattern suggests that debonding or a fracture at the cervical region greater than root fracture in the apical region could be the cause of a failure in the tooth model repaired with GF/PBA-a composite post. Furthermore, it was also observed that the stress pattern of the tooth model repaired with the developed composite post with more than 23.5 vol% GF (Figures 7(c)-7(d)) showed much similarity to the tooth model repaired with the commercial one (Figure 7(f)).

Stress patterns of the σ_v, resulted from an applied vertical load of 100 N, along cross-section A to H (from Figure 8a) for tooth model repaired with composite posts and along cross section

A to F (from Figure 8b) for natural tooth model, are presented in Figure 9. It was observed that the stress distribution within the composite post reinforced with 65.1 vol% GF showed the largest amount of σ_v, followed by 41.2 vol% GF and 23.7 vol% GF, respectively; the 10.5 vol% GF/PBA-a composite post showed the lowest amount of σ_v. According to these findings, the post with a larger elastic modulus generated a higher concentration of stress and were found to amplify tension within the post, which decreased stress in the root dentin.[47,48] Lower stress in dentin is beneficial because it increases resistance of dentin to greater cyclic loading and lower the likelihood of root failure. At the dentin-composite resin-post interface (location in a range of 2.49-3.09 mm in Figure 8a) of the tooth model repaired with the posts, i.e., GF/poly(BA-a) composites and commercial GF posts showed similar stress patterns as in the natural tooth model. It is possible that the post's elastic modulus was comparable to that of the dentin (18.6-40 GPa)[15,16] and the composite resin (16.6 GPa),[34] in consequence, the stress distributions across the interfaces were nearly constant.

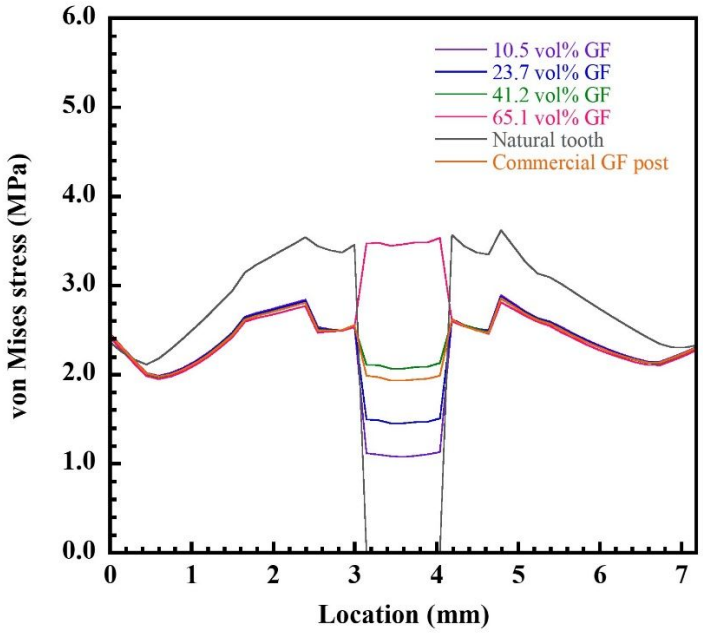

FIGURE 9 σ_v distributions generated across the line A-H and line A-F of the root in tooth model repaired with posts, i.e., GF/PBA-a composite posts and commercial GF post[36], and the natural tooth model, respectively.

3.5 Chemical formation of GF/PBA-a composites

The characteristics of the GF/PBA-a composite might be significantly influenced by the quality of the interfacial bonding. FTIR provides great potential to monitor the chemical interactions between GF and PBA-a, hence measurements were performed, and the obtained spectra are illustrated in Figure 10. Figures 10a and 10b, show the FTIR spectra of the GF as received, and

that of heat-treated GF which were found to quite similar indicating that the GF without any chemical treatment was used in this work. For GF, the absorption peaks at 1000 cm^{-1} and 900 cm^{-1} were presented and allocated to the symmetric stretching and bending vibrations of the siloxane group (Si–O–Si), respectively. An absorption peak at 1400 cm^{-1} was also detected and pointed to the symmetric stretching of other oxides, i.e., aluminum oxide, boron oxide and so on.[49-51]

In Figure 10c, the aromatic ether (C–O–C stretching) for an oxazine ring of the BA-a was provided the absorption peak at 1230 cm^{-1} and the tri-substituted benzene ring was identified at 935 cm^{-1} and 1488 cm^{-1}. These absorption peaks were totally vanished following heat treatment, indicating complete oxazine-ring opening of the BA-a, in a consequence, the absorption peaks at 878 cm^{-1} and 1477 cm^{-1} identified the tetra-substituted aromatic ring[52,53] in Figure 10d was obtained. Furthermore, a broad peak about 3380 cm^{-1} could be used to monitor the signature of the ring-opening reaction of the BA-a during heat cure. This peak is attributed to the synthesis of phenolic hydroxyl groups (O–H), which can further interact to the GF.

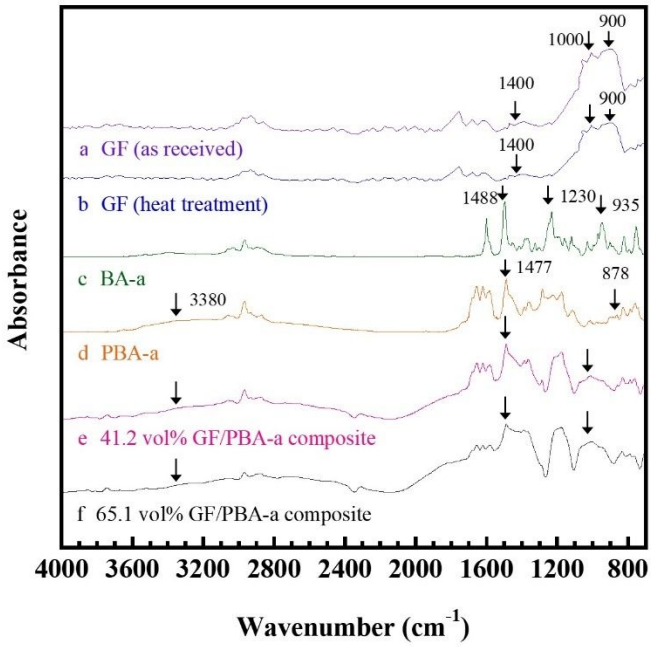

FIGURE 10 FTIR spectra: **a** GF as received, **b** heat treated GF, **c** BA-a, **d** PBA-a, **e** 41.2 vol% GF/PBA-a composite, **f** 65.1 vol% GF/PBA-a composite.

The network formed between the PBA-a and the GF of the GF/PBA-a composite reinforced with 41.2 vol% and 65.1 vol% GF was also studied by FTIR spectroscopy, and their spectra are shown in Figures 10e and 10f. The characteristic peaks of GF and PBA-a were also presented in the FTIR spectra of the composites. Furthermore, it was seen that the height of the absorption peak at 3380 cm^{-1} which was the characteristic of phenolic moiety of PBA-a tended

to decrease for the PBA-a composites reinforced with 41.2 vol% and 65.1 vol%; as expected, the phenolic moiety further interacted with the GF in the formation of hydrogen bonding (O–H···O) between the hydroxyl groups of PBA-a (O–H groups) and the oxygen atom of GF (---O–Si–O–Si–) as the hydrogen bond at absorption peaks of 2800-1800 cm^{-1} was indicated.

Figure 11 depicts a potential chemical interaction between the GF and the PBA-a. Figure 11a presents the BA-a oxazine ring which was opened by heat cure and formed the phenolic moiety. Then, hydrogen bonds were formed when the phenolic hydroxyl group reacted with the GF to form the linkages in the polymer networks, as suggested in Figure 11b. The formation of linkages resulted in good interfacial adhesion between the GF surface (Figure 11c) and the PBA-a matrix. As seen from the fracture surface topography of the GF/PBA-a composite in Figure 11d, long GF pull-out, GF breaking pattern and debonding gaps between the GF and the PBA-a matrix were not observed.

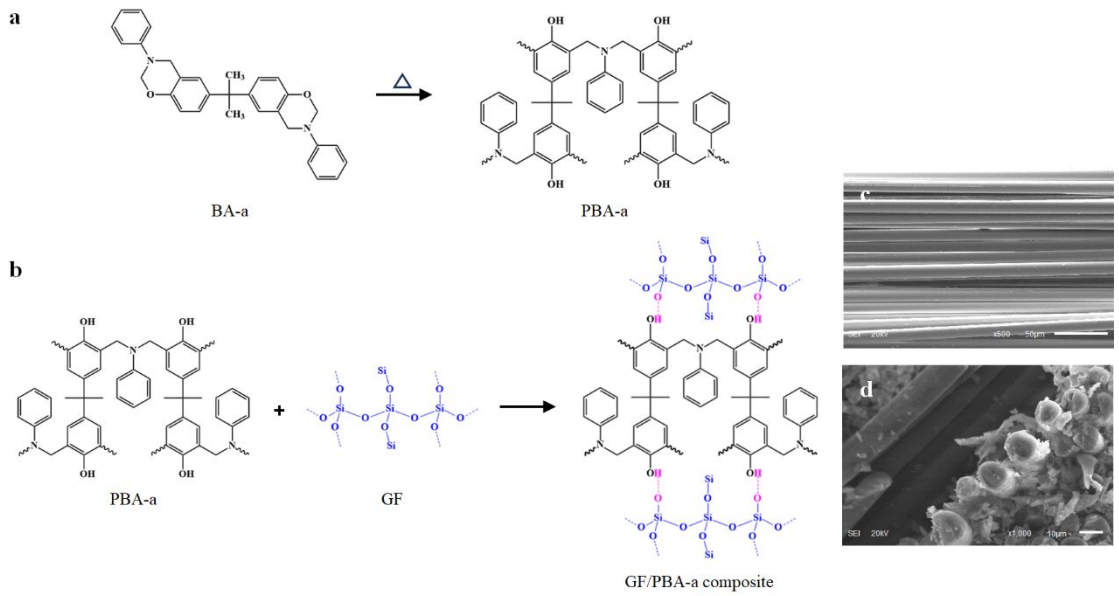

FIGURE 11 a Polymerization reaction of BA-a, **b** A possible chemical reaction between PBA-a and GF, **c** glass fiber as received, **d** fracture surface of 65.1 vol% GF/PBA-a composite.

4 CONCLUSIONS

The influence of GF loading on thermal expansion, thermal stability, and biocompatibility of the GF-reinforced PBA-a composites for dental fiber post can be summarized as follows: the CTE of PBA-a was constant in the temperature range 20 °C-150 °C, and it can be significantly decreased to match the CTE of dentin using a GF loading of 65.1 vol%. The degradation temperature of the PBA-a composites was improved by GF reinforcement, in the temperature range from 325 °C-391 °C, which was significantly higher from the thermal loading situations

developed on teeth, such as teeth restoration, food consumption and dental treatment. In addition, the PBA-a composites were found to be biocompatible materials as cell viability was found to be more than 90 %. The tooth model repaired with GF/PBA-a composite posts was subjected to FEA to examine the stress distribution. The results indicated that the dentin experienced the lowest stress magnitude in the case of the 65.1% GF/PBA-a composite post. Based on this evidence, it can be suggested that the 65.1 vol% GF/PBA-a composite post with improved thermal expansion and thermal stability as well as cytocompatibility would have great potential for applications in dentistry including manufacturing of endodontic posts. Future work will explore additional eco-friendly features in order to examine the feasibility of utilizing bio-based PBA-a for GF posts.

AUTHOR CONTRIBUTIONS

Phattarin Mora: Methodology, formal analysis, data curation, writing-original draft preparation. Sarawut Rimdusit: Validation, writing-review and editing. Panagiotis Karagiannidis: Writing-review and editing. Ukrit Srisorrchart: Validation. Chanchira Jubsilp: Conceptualization, methodology, validation, formal analysis, data curation, writing-review and editing, supervision, funding acquisition.

ACKNOWLEDGMENTS

The funding for this study has come from the NSRF via the Program Management Unit for Human Resources and Institutional Development, Research and Innovation (grant number B05F640094), the National Research Council of Thailand (NRCT) and Srinakharinwirot University (grant number N42A650377), Srinakharinwirot University Development (grant number 588/2565), the National Research Council of Thailand (NRCT) and Chulalongkorn University (grant number N42A660910).

CONFLICT OF INTEREST STATEMENT

The authors declare no conflict of interest.

DATA AVAILABILITY STATEMENT

The data that support the findings of this study are available from the corresponding author upon reasonable request.

REFERENCES

1. Mariana Desireé Reale Batista MD, Drzal LT, Kiziltas A, Mielewski D. Hybrid cellulose-inorganic reinforcement polypropylene composites: lightweight materials for automotive applications. *Polym Compos*. 2019;41:1074-1089. doi:10.1002/pc.25439
2. Irez AB, Yakar H. Transformation of waste carbon fiber prepreg into sustainable composites: application in the automotive industry components. *Polym Compos*. 2024;1-16. doi:10.1002/pc.28421
3. de Melo Morgado GF, Montagna LS, Gouvêa RF, Guimarães A, Passador FR, Rezende MC. Fatigue resistance of carbon fiber/polyphenylene sulfide composites engineered for automotive use. *Polym Compos*. 2024;45:7719-7733. doi:10.1002/pc.28299
4. İskender Özsoy M. Investigation of the energy absorption behavior and damage mechanisms of aramid/carbon/jute fiber hybrid epoxy composites. *Polym Compos*. 2024;1-17. doi:10.1002/pc.28583
5. Ojha S, Bisaria H, Mohanty S, Kanny K. Fractographic analysis of fiber-reinforced polymer laminate composites for marine applications: A comprehensive review. *Polym Compos*. 2024;45: 6771-6787. doi:10.1002/pc.28271
6. Mora P, Okhawilai M, Jubsilp C, Bielawski CW, Rimdusit S. Glass fabric reinforced polybenzoxazine composites filled with nanosilica: A High impact response poises use as strike panels in multilayered armor applications. *J Mater Res Technol*. 2020;9:12723–12736. doi:10.1016/j.jmrt.2020.09.005
7. Arpitha GR, Verma A, Sanjay MR, Siengchin S. Preparation and experimental investigation on mechanical and tribological performance of hemp-glass fiber reinforced laminated composites for lightweight applications. *Adv Civ Eng Mater*. 2021;10:427-439. doi:10.1520/ACEM20200187
8. Arpitha GR, Jain N, Verma A. Banana biofiber and glass fiber reinforced hybrid composite for lightweight structural applications: mechanical, thermal, and microstructural characterization. *Biomass Convers Biorefin*. 2024;14:12589–12598. doi:10.1007/s13399-023-04300-y
9. Sakaguchi RL, Ferracane J, Powers JM. Fundamentals of materials science, in: *Craig's Restorative Dental Materials*. Elsevier; 2012.
10. Chieruzzi M, Pagano S, Cianetti S, Lombardo G, Kenny JM, Torre L. Effect of fibre posts, bone losses and fibre loading on the biomechanical behaviour of endodontically treated teeth: 3D-finite element analysis. *Mater Sci Eng C*. 2017;74:334-346. doi:10.1016/j.msec.2016.12.022

11. Baldea B, Silaghi-Dumitrescu L, Furtos G. Fracture load and force load at upper yield of alkaline-resistant glass fiber-reinforced endodontic posts. *Polym Compos*. 2015;38:260-267. doi: 10.1002/pc.23583
12. Lamichhane A, Xu C, Zhang FQ. Dental fiber-post resin base material: a review. *J Adv Prosthodont*. 2014;6:60-65. doi:10.4047/jap.2014.6.1.60
13. Toparli M. Stress analysis in a post-restored tooth utilizing the finite element method. *J Oral Rehabil*. 2003;30:470-476. doi:10.1046/j.1365-2842.2003.01090.x
14. Penelas AG, da Silva EM, Poskus LP, Alves AC, Simões IIN, Hass V, Guimarães JGA. Development and characterization of biological bovine dentin posts. *J Mech Behav Biomed Mater*. 2019;92:197-205. doi:10.1016/j.jmbbm.2019.01.018
15. Novais VR, Quagliatto PS, Bona AD, Correr-Sobrinho L, Soares CJ. Flexural modulus, flexural strength, and stiffness of fiber-reinforced posts. Indian J Dent Res. 2009;20:277-281. doi: 10.4103/0970-9290.57357
16. Bateman G, Ricketts DN, Saunders WP. Fibre-based post systems: A review. *Br Dent J*. 2003;195:43-48. doi:10.1038/sj.bdj.4810278
17. Moosavi H, Maleknejad F, Kimyai S. Fracture resistance of endodontically-treated teeth restored using three root-reinforcement methods. *J Contemp Dent*. 2008;9:30-37.
18. Zicari F, Coutinho E, Scotti R, Meerbeek BV. Naert I. Mechanical properties and micro-morphology of fiber posts. *Dent Mater*. 2013;29:e45–e52. doi:10.1016/j.dental.2012.11.001
19. Cheleux N, Sharrock PJ. Mechanical properties of glass fiber-reinforced endodontic posts. Acta Biomater. 2009;5:3224-3230. doi:10.1016/j.actbio.2009.04.008
20. Lassila LVJ, Tanner J, Bell AML, Narva K, Vallittu P K. Flexural properties of fiber reinforced root canal posts. *Dent Mater*. 2004;20:29-36. doi:10.1016/s0109-5641(03)00065-4
21. Pegoretti A, Fambri L, Zappini G, Bianchetti M. Finite element analysis of a glass fibre reinforced composite endodontic post. *Biomaterials*. 2002;23:2667-2682. doi:10.1016/s0142-9612(01)00407-0
22. Tekin S, Adiguzel O, Cangul S, Atas O, Erpacal B. Evaluation of the use of PEEK material in post-core and crown restorations using finite element analysis. *Am J Dent*. 2020;33:251-257.
23. Yang A, Xu C. Synthesis and characterization of a polyimide-epoxy composite for dental applications. *Mech Compos Mater*. 2018;54:71-78. doi:10.1007/s11029-018-9719-7

24. Sukanto H, Raharjo WW, Ariawan D, Triyono J, Kaavesina M. Epoxy resins hermosetting for mechanical engineering. *Open Engineering* 2021;11:797–814. doi:10.1515/eng-2021-0078
25. Kurihara S, Idei H, Aoyagi Y, Kuroe M. Binder Resin for Friction Material, Binder Resin Composition for Friction Material, Composite Material for Friction Material Containing the Same, Friction Material and Production Method Thereof. US8227390B2, 24 July 2012.
26. Mora P, Nunwong C, Sriromreun P, Kaewsriprom P, Srisorrachatr U, Rimdusit S, Jubsilp C. High performance composites based on highly filled glass fiber-reinforced polybenzoxazine for post application. *Polymers*. 2022;14: 4321. doi:10.3390/polym14204321
27. Ishida H. Process for preparation of benzoxazine compounds in solventless systems. US Patent 5,543,516, 6 Aug 1996.
28. Rimdusit S, Jubsilp C, Tiptipakorn S. *Alloys and Composites of Polybenzoxazines*. Springer; 2013.
29. Ishida H, Agag T. *Handbook of Benzoxazine Resins*. Elsevier; 2011.
30. Ishida H, Froimowicz P. *Advanced and Emerging Polybenzoxazine Science and Technology*. Elsevier; 2017.
31. Repetto G, del Peso A, Zurita JL. Neutral red uptake assay for the estimation of cell viability/cytotoxicity. *Nat Protoc*. 2008;3:125-1131. doi:10.1038/nprot.2008.75
32. Ko C, Chu C, Chung K, Lee M. Effects of posts on dentin stress distribution in pulpless teeth. *J Prosthet Dent*. 1992;68:421–427. doi:10.1016/0022-3913(92)90404-x
33. de Coelho CSM, Biffi JCG, da Silva GR, Abrahao A, Campos RE, Soares CJ. Finite element analysis of weakened roots restored by composite resin and posts. *Dent Mater J*. 2009;28:671-678. doi:10.4012/dmj.28.671
34. Chatvanitkul C, Lertchirakarn V. Stress distribution with different restorations in teeth with curved roots: A finite element analysis study. *J Endod*. 2010;36:115-118. doi:10.1016/j.joen.2009.09.026
35. Genovese K, Lamberti L, Pappalettere C. Finite element analysis of a new customized composite post system for endodontically treated teeth. *J Biomech*. 2005;38:2375-2389. doi:10.1016/j.jbiomech.2004.10.009
36. Lanza A, Aversa R, Rengo S, Apicella D, Apicella A. 3D FEA of cemented steel, glass and carbon posts in a maxillary incisor. *Dent Mater*. 2005;21:709–715. doi:10.1016/j.dental.2004.09.010

37. Chu XX, Wu ZX, Huang RJ, Zhou Y, Li LF. Mechanical and thermal expansion properties of glass fibers reinforced PEEK composites at cryogenic temperatures. *Cryogenics*. 2010;50:84-88. doi:10.1016/j.cryogenics.2009.12.003
38. Jacobs MJN, Dingenen JLJV. Ballistic protection mechanisms in personal armour. *J Mater Sci*. 2001;36:3137–3142. doi:10.1023/A:1017922000090
39. Kimura H, Matsumoto A, Ohtsuka K. Glass fiber-reinforced composite based on benzoxazine resin. *J Appl Polym Sci*. 2009;114:1256–1263. doi:10.1002/app.30427
40. Hengchang X, Wenyi L, Tong W. Measurement of thermal expansion coefficient of human teeth. *Aust Dent J*. 1989;34:530-535. Doi:10.1111/J.1834-7819.1989.TB04660.X
41. Luiz BKM, Amboni DRMC, Prates LHM, Bertolino JR, Pires ATM. Influence of drinks on resin composite: Evaluation of degree of cure and color change parameters. *Polym Test*. 2007;26:438-444. doi:10.1016/j.polymertesting.2006.12.005
42. Lohbauer U. Dental glass ionomer cements as permanent filling materials? – properties, limitations and future trends. *Materials*. 2010;3:76-96. doi:10.3390/ma3010076
43. Wang T, Matinlinna JP, Burrow MF, Ahmed KE. The biocompatibility of glass-fibre reinforced composites (GFRCs) - a systematic review. *J Prosthodont Res*. 2021;65:273-283. doi:10.2186/jpr.JPR_D_20_00031
44. Allen RJ, Waclaw B. Bacterial growth: a statistical physicist's guide. Rep Prog Phys. 2019;82:016601. doi:10.1088/1361-6633/aae546
45. Dadsetan M, Pumberger M, Casper ME, Shogren K, Giuliani M, Ruesink T, Hefferan TE, Currier BL, Yaszemski MJ. The effects of fixed electrical charge on chondrocyte behavior. *Acta Biomater*. 2011;7:2080-2090. doi:10.1016/j.actbio.2011.01.012
46. Thevenot P, Hu W, Tang L. Surface chemistry influences implant biocompatibility. *Curr Top Med Chem*. 2008;8:270-280. doi:10.2174/156802608783790901
47. Asmussen E, Peutzfeldt A, Sahafi A. Finite element analysis of stresses in endodontically treated, dowel-restored teeth. *J Prosthet Dent*. 2005;94:321-329. doi:10.1016/j.prosdent.2005.07.003
48. Joshi S, Mukherjee A, Kheur M, Mehta A. Mechanical performance of endodontically treated teeth. *Finite Elem Ana. Des*. 2001;37:587-601. doi:10.1016/S0168-874X(00)00059-7
49. Bonon AJ, Weck M, Bonfante EA, Coelho PG. Physicochemical characterization of three fiber-reinforced epoxide-based composites for dental applications. *Mater Sci Eng C*. 2016;69:905–913. doi:10.1016/j.msec.2016.07.002

50. Moreno-Maldonado V, Acosta-Torres LS, Barcelo-Santana FH, Vanegas-Lancon RD, Plata-Rodrı´guez ME, Castano VM. Fiber-reinforced nanopigmented poly(methyl methacrylate) as improved denture base. *J Appl Polym Sci*. 2012;126:289-296. doi:10.1002/app.36913
51. Nandiyanto ABD, Oktiani R, Ragadhita R. How to read and interpret FTIR spectroscope of organic material. *Indones J Sci Technol*. 2019;4:97-118. doi:10.17509/ijost.v4i1.15806
52. Takeichi T, Guo Y, Agag T. Synthesis and characterization of poly(urethane-benzoxazine) films as novel type of polyurethane/phenolic resin composites. *J Polym Sci Part A: Polym Chem*. 2000;38:4165-4176. doi:10.1002/1099-0518(20001115)38:22<4165::AID-POLA170>3.0.CO;2-S
53. Mora P, Jubsilp C, Bielawski CW, Rimdusit S. Impact response of aramid fabric-reinforced polybenzoxazine/urethane composites containing multiwalled carbon nanotubes used as support panel in hard armor. *Polymers* 2021;13:2779. doi:10.3390/polym13162779

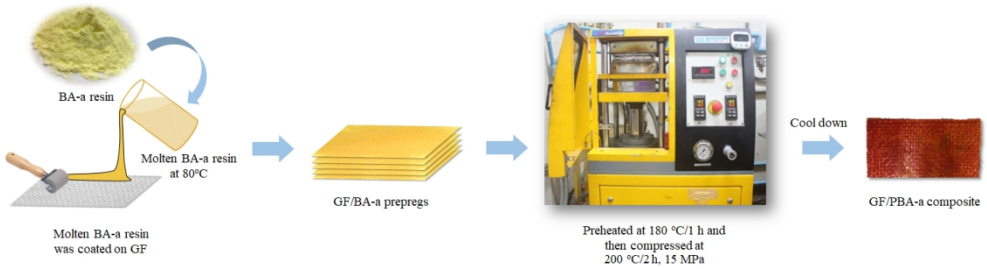

123x34mm (300 x 300 DPI)

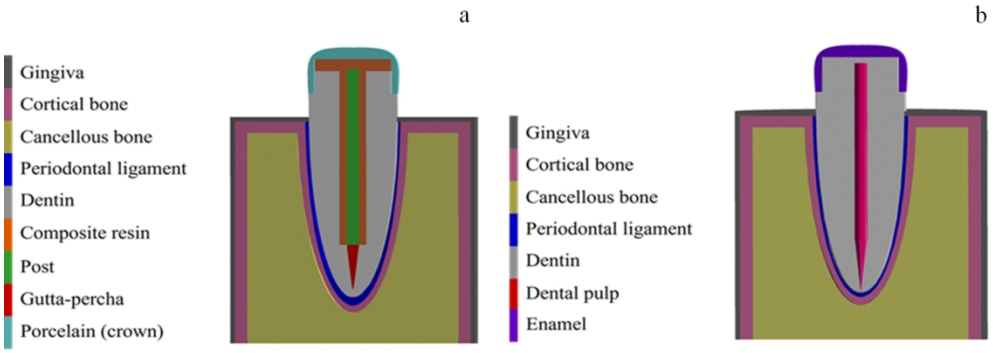

124x44mm (300 x 300 DPI)

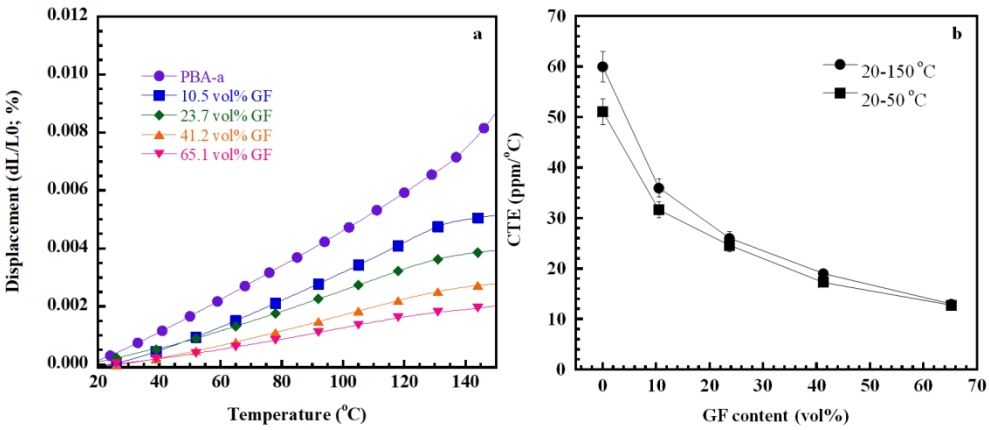

141x62mm (300 x 300 DPI)

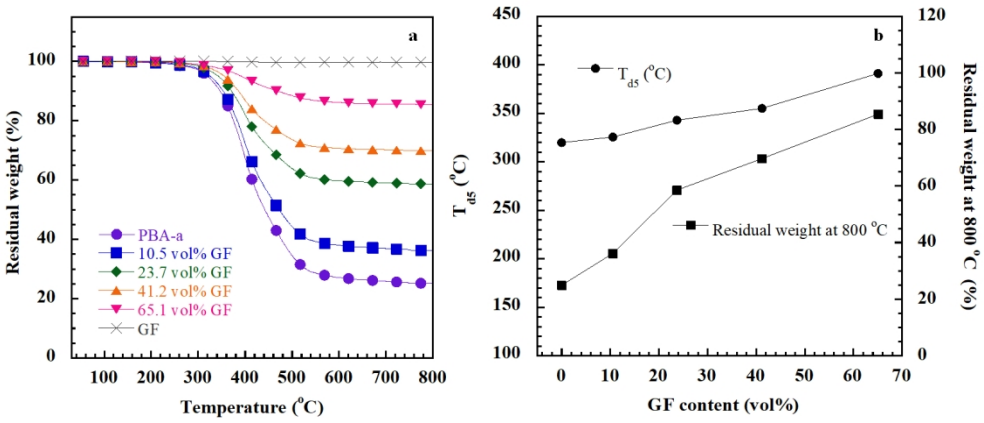

144x61mm (300 x 300 DPI)

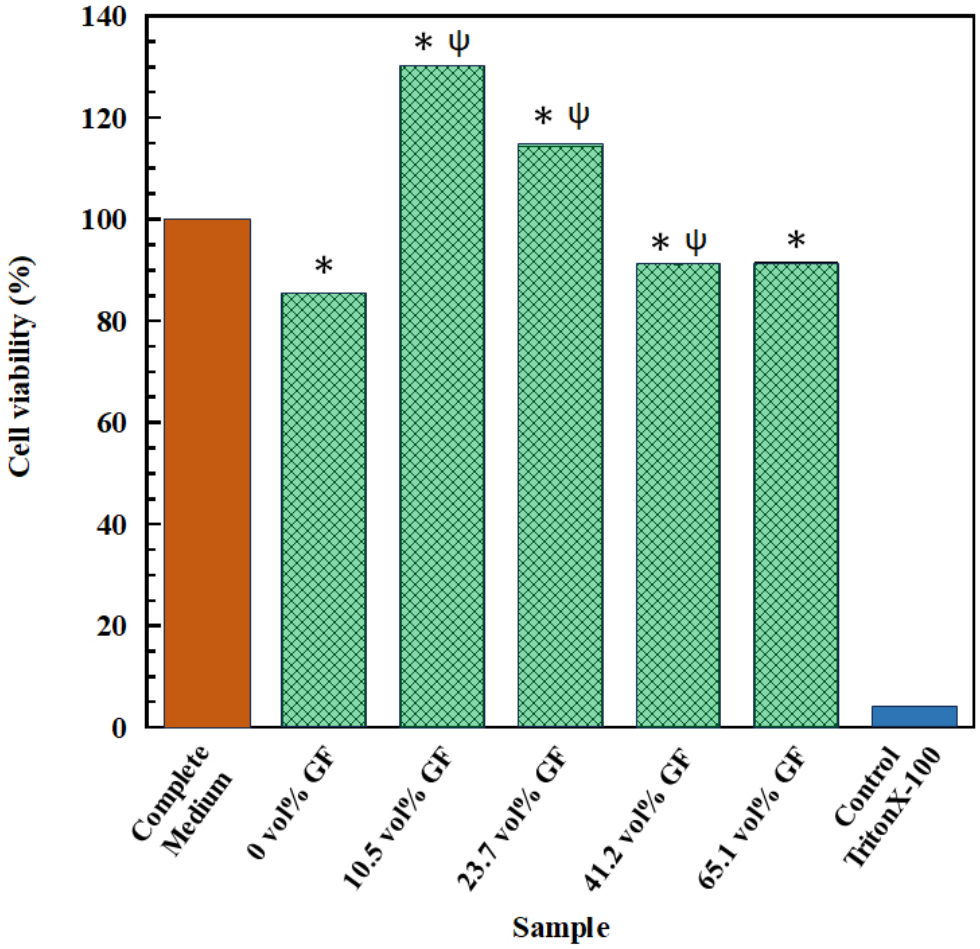

62x60mm (300 x 300 DPI)

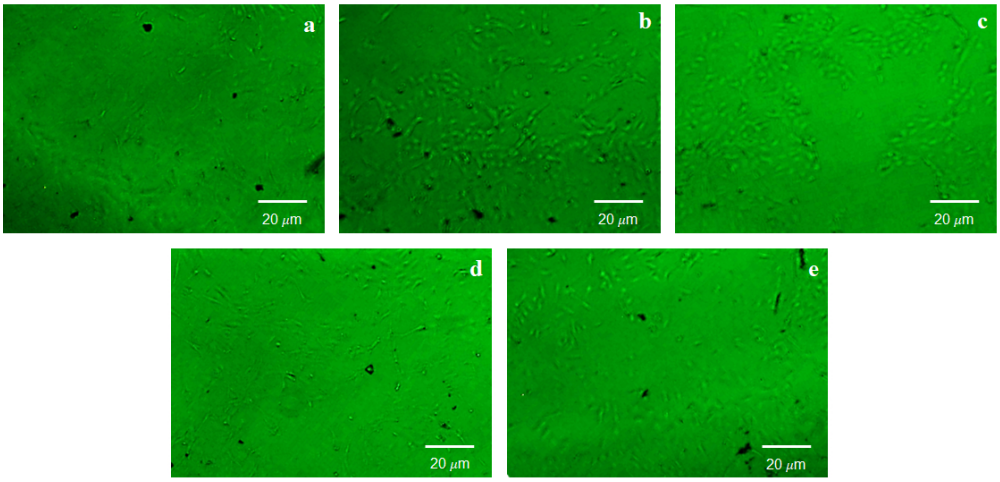

94x45mm (300 x 300 DPI)

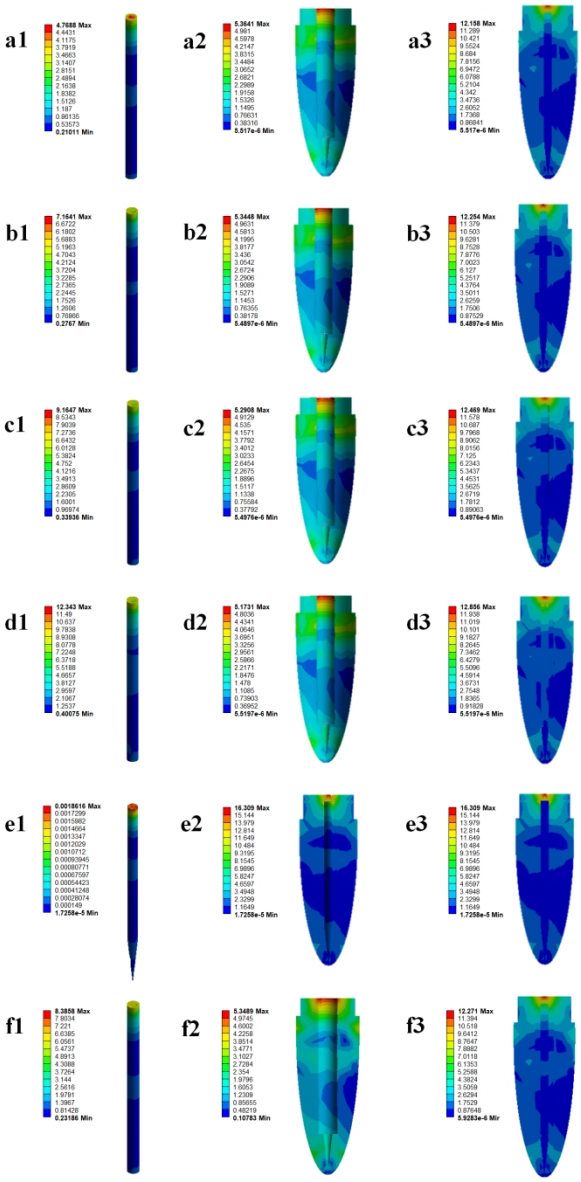

120x224mm (300 x 300 DPI)

a

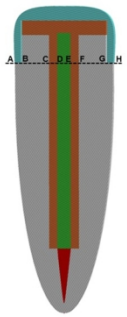

Path key point	Local coordinate (mm)
A	0.00
B	0.50
C	2.49
D	3.09
E	4.09
F	4.69
G	6.68
H	7.18

b

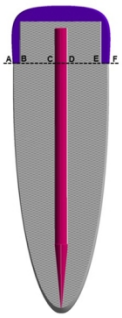

Path key point	Local coordinate (mm)
A	0.00
B	0.05
C	3.09
D	4.09
E	6.68
F	7.18

139x59mm (300 x 300 DPI)

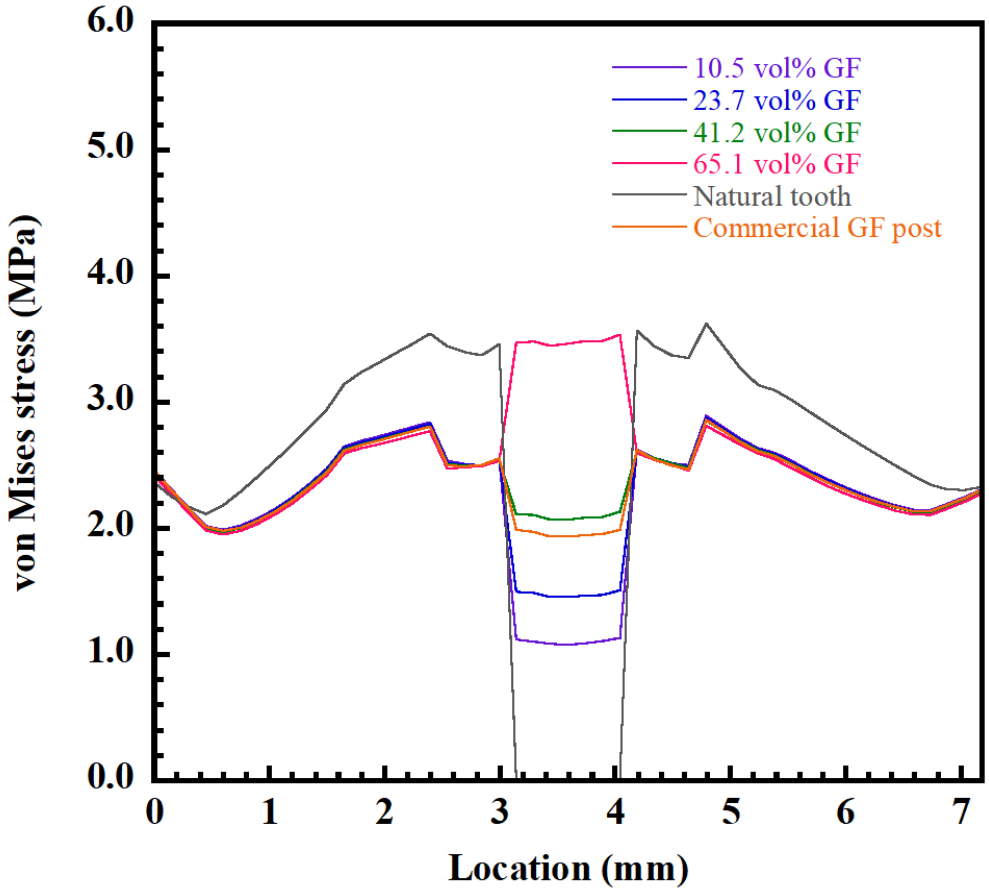

81x73mm (300 x 300 DPI)

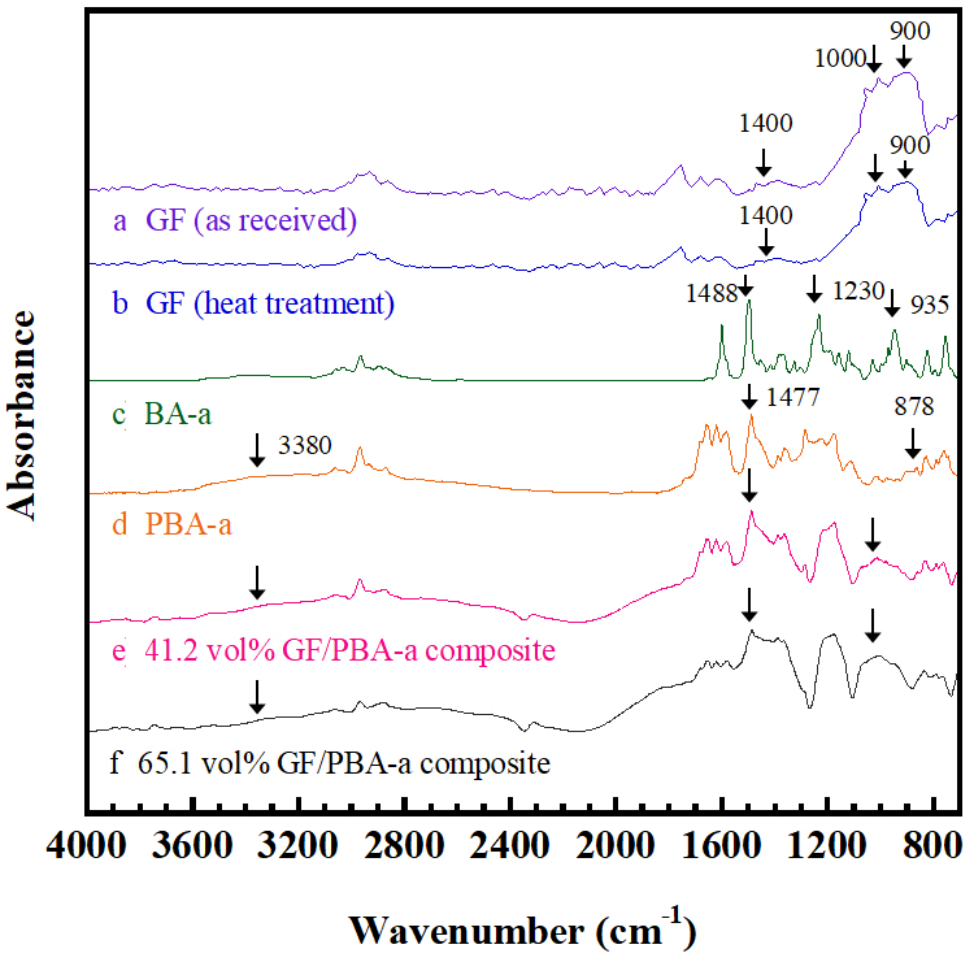

65x63mm (300 x 300 DPI)

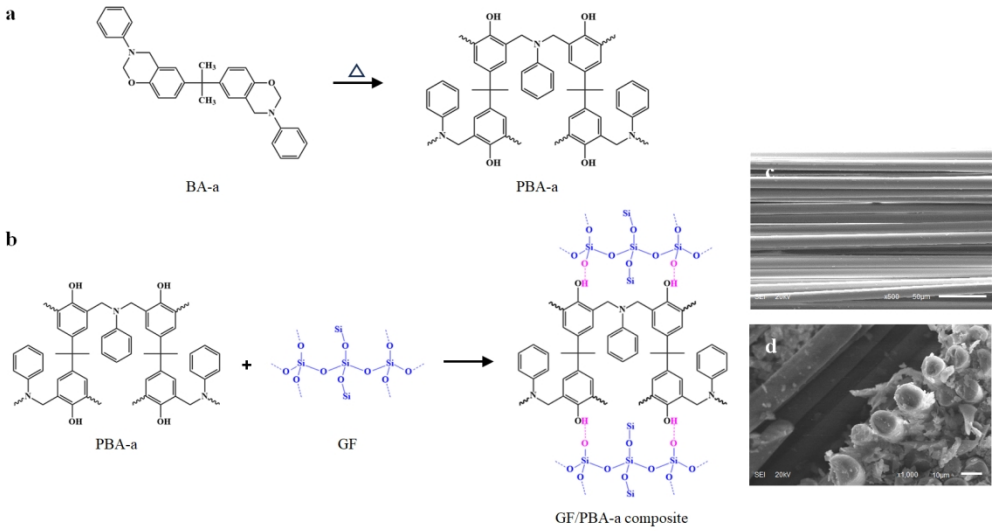

147x80mm (300 x 300 DPI)